BENCHMARKING OF CFRP STRUCTURES IN THE PRELIMINARY OVERALL DESIGN OF CIVIL TRANSPORT AIRCRAFT

J.Rieke*, W.Heinze, P.Horst
Institute of Aircraft Design and Lightweight Structures (IFL), TU Braunschweig
Hermann-Blenk-Str. 35, 38104 Braunschweig, Germany

ABSTRACT

The impact of CFRP structures on the overall design of different civil transport aircraft is presented in the context of multidisciplinary, integrated preliminary design studies with the preliminary aircraft design and optimization tool (PrADO). The PrADO process chain is described with a focus on the structural sizing module, which has been improved by the ability to handle layered composite materials. Therefore the implementation of a failure criterion in a modified fully stressed design process is highlighted. Furthermore, the positive and negative impacts on economy (DOC) and environment (fuel consumption) are pointed out by the integrated approach. Hence, the overall design results of a typical short range and a typical long range aircraft, both with primary CFRP wing structures, are discussed to indicate whether and for which aircraft type – short range or long range – an advantage can be found.

NOTATION

ν	Poisson ratio
σ	Stress
τ	Shear stress
f_E	Lamina exertion
f_E^*	Modified lamina exertion
n	Acceleration in z-direction
p	Incline parameter
t	Wall thickness
B	Width
E	Young's modulus
G	Shear modulus
H	Height
K	Notch factor
L	Length
R	Strength, fracture resistance
S	Thrust
Ma_C	Cruise Mach number

Indices

$\|\|$	Fiber parallel
$\perp$	Fiber transverse
$\perp\perp$	Transverse-transverse
$\perp\|\|$	Transverse-parallel
1, 2, 21	Layer coordinate system: parallel, transverse, transverse-parallel
+	Tension
-	Compression
a	Allowable
e	Element
A	Action plane

ABBRAVIATIONS

CFRP	Carbon Fiber Reinforced Plastic
FF	Fiber Failure
FRP	Fiber Reinforced Plastic
IFF	Inter Fiber Failure
L/D	Lift to drag ratio
MLW	Maximum Landing Weight
MTOW	Maximum Take Off Weight
OEW	Operating Empty Weight

1 MOTIVATION

Fibre reinforced plastics (FRP) play an exceeding role in present aircraft projects (Boeing 787, Airbus A350) and it can be expected that the primary structures of future aircraft projects will be designed also of FRP since these have more potential to influence significantly the structure mass and the deformation behaviour having regard to aeroelastics [1] in comparison to metals.

While the integrated multidisciplinary design process for civil aircraft contains sequential and mostly iterative computations, which take into account the complexity of the aircraft system with the high amount interaction between the disciplines [2, 3, 4], the requirements on a sizing procedure for FRP structures are mainly restrained by two demands:

On the one hand it has to be fast due to the iterative character of the preliminary design process, which should allow extensive parameter studies or optimization of an aircraft configuration.

On the other hand the sizing procedure has to be conservative. This is very important especially for preliminary design, because in an early design phase many uncertainties (e.g. load combinations, manufacturing issues) exist and can not be foreseen [5]. Further it has to be precise enough to represent the physics correct and avoids therefore an oversized structure with weight lacks.

Regarding these requirements the structural sizing module of the multidisciplinary design and optimization tool PrADO has been enhanced. The next chapter describes the mode of operation, the architecture of PrADO and in detail of the structural, aerodynamic and aeroelastic sizing module (SAM), to understand the global relation of the

* corresponding author; j.rieke@tu-bs.de; fon: 0531-3919912; fax. 0531-3919904

structural sizing module in the overall aircraft design with PrADO.

2 PRELIMINARY AIRCRAFT DESIGN AND OPTIMISATION TOOL – PRADO

PrADO has been under development for over 20 years at the Institute of Aircraft Design and Lightweight Structures (IFL) as a multidisciplinary integrated design tool for estimation of all aircraft aspects in the preliminary phase [6, 7]. The spectrum of representable configurations ranges from conventional transport aircraft [8] over blended wing bodies [9] to unconventional aircraft [10].

2.1 PrADO Design Process

To cover the multidisciplinary approach, PrADO features a highly modular structure, which enables one to integrate easily new methods of different fidelities. In **Fig. 1** a simplified overview of the PrADO structure with its subordinated design modules, ordered by the specific disciplines, is depicted. These modules are linked by a data base management system (DMS), in which all configuration data are thematically stored and therefore are made accessible to all modules.

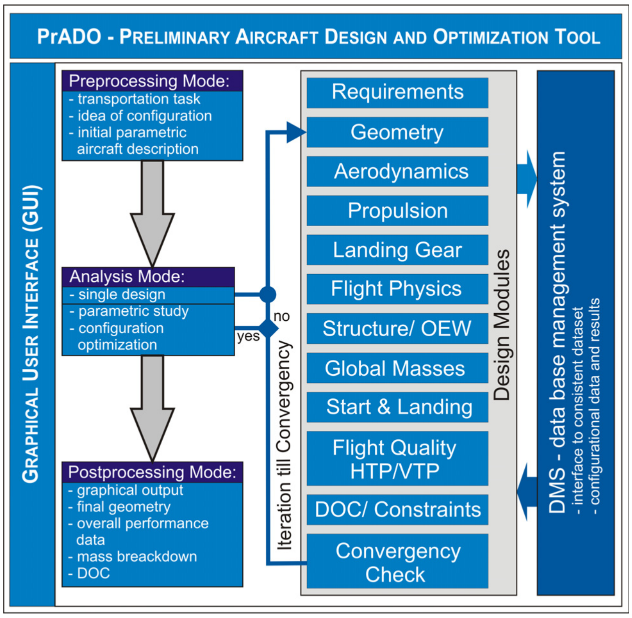

Fig. 1: PrADO Process Chain

In the preprocessing mode of PrADO an input file has to be generated by the user. This input file contains independent data from a zero level aircraft design and covers numerous design requirements (e.g. ranges, transport mission, configuration, parametric geometric data, cabin layout, etc.) for an initial parametric definition of the aircraft.

In the analysis mode the user can choose between three different analysis types. The single design analysis represents the core type. It processes iteratively the complete sequence of design modules until convergence of all dependent design parameters is fulfilled. Thereby, the dependent design variables form the response quantities of different design modules (e.g. current operating empty weight). The parametric study enables the user to vary specific independent variables within a range of interest to get an overview of the design space. Hence, for every variable set a single analysis has to be performed, which is automatically repeated in this mode within the range of the parameters. A parametric study consequently consists of several single design analyses. In this point the optimization mode is similar to the parametric study. But hereby it is necessary to define a target function (e.g. OEW) and boundary conditions, so that an optimization algorithm can process gradients between the single analyses. With these gradients the independent design variables are modified and a new single analysis is started until the target function is fulfilled.

The single analysis process is organized as followed: The requirements of the input data are interpreted in the first module and are distributed into the object ordered data bases. Then the iterative aircraft design process (cp. Fig. 1) starts with the geometry module, which analyses the parametric, geometric input data and calculates the missing data to describe the aerodynamic surface, the structural design and interior of all aircraft components. This module is subdivided into different modules, each for one aircraft component (e.g. fuselage, wing), so that additional aircraft components like external tanks can be added via an extra module.

In the aerodynamics module the aerodynamic data characteristics for the different flight and loading cases are calculated for the whole configuration. For this purpose different types of steady aerodynamic codes are available (e.g. lifting line code: Lifting Line [11], panel code: HISSS (EADS-M, [12])). The results are necessary for flight simulation (predicting performance), control and stability properties (flight physics, start & landing, HTP/VTP flight quality modules).

The propulsion module computes the engine characteristics – including a weight and geometry estimation – by simulating the thermodynamic cycle for a turbo-fan engine. These data are needed besides the aerodynamic characteristics to evaluate the flight physics of the aircraft configuration.

In the landing gear module the load classification number (LCN), the load factor and the sizing are performed by handbook methods (cp. [6]).

The structural mass can be computed by a range of methods with different levels of fidelity, which go from the semi empiric and statistical methods (e.g. *Burt-Philips* [13], *Driggs* [14]) over analytical beam models to a method based on the FE method (SAM [7]). Where the simple methods do not need aerodynamic loads, the analytical beam method derives aerodynamic loads from Lifting Line [11] for defined load cases. SAM, which is described in detail in chapter 2.2, calculates the loads for different load cases with HISSS [12].

The structural mass results are needed by the following module to compose the component masses together with operational items, airframe services and equipment to the operational empty weight (OEW). Also, the global masses (e.g. MTOW, MLW) are computed.

In the flight quality modules the vertical and horizontal tail plane effectiveness for control and stability are verified.

Finally the direct operation costs (DOC) are computed and the design constraints are checked for compliance. If the convergence check of the dependent parameters is negative, a new iteration loop is started until convergence is reached.

2.2 Structural Aerodynamic and Aeroelastic Sizing Module

The module in which PrADO calculates the structural mass is called the structural aerodynamic and aeroelastic sizing module (SAM, based on work of *Österheld* [7]). Its primary function is a physics-based computation of the primary structural masses: fuselage, wing, horizontal tail plane (HTP) and vertical tail plane (VTP).

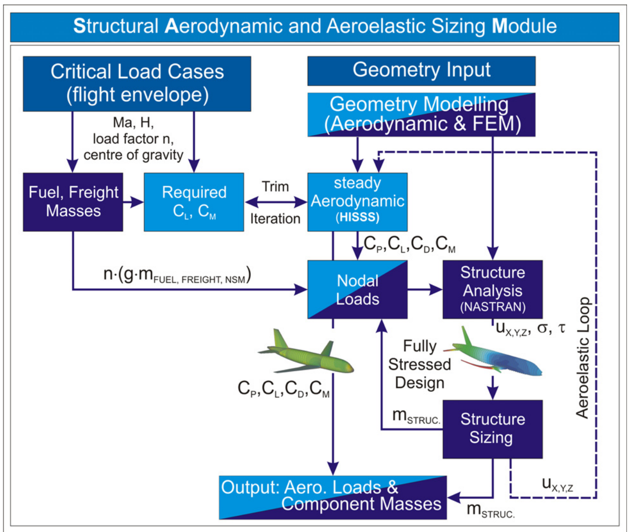

Fig. 2: Structural Aerodynamic and Aeroelastic Sizing Module

Corresponding to **Fig. 2**, first of all critical load cases are specified by the maneuver and gust flight envelope corner points (according to FAR25 specifications) for different flight attitudes. These are characterized by specific loading conditions (fuel and payload distribution ⇒ center of gravity, aircraft weight), altitude and Mach number. The flight loads therefore are derived from a steady aerodynamic calculation with HISSS (cp. [12]), which is iterated until the required lift coefficient C_L and moment coefficient C_M are obtained for each load case. The aerodynamic loads are compensated by inertia forces (structure, payload, secondary masses). In addition to the flight load cases landing impact cases are specified. Under consideration of the dynamic behavior of the landing gear spring damper system, the maximum landing gear reaction forces are computed for a 10 ft/s landing impact. The corresponding acceleration is applied as an inertia load to all mass points and the structure.

The HISSS calculation needs a geometrical description of the aerodynamic surface of the aircraft, which is provided by a submodule called multi model generator (MMG). During the first step the MMG generates a splined surface of the aircraft surfaces (non-uniform rational B-splines, NURBS), based on the PrADO geometry description. Corner points for the aerodynamic panels are extracted from the NURBS geometry and stored in the HISSS mesh input file format.

The structural model for the finite element method (FEM) is composed in a similar way. The location of e.g. the wing box or the fuselage frames is determined by the PrADO database and the precise node location can be interpolated from the NURBS description. In this way the nodes and elements are built up for all primary structure parts. The property entries of the FE-model are also generated by the MMG from PrADO input file data and are written to a special data base. Non structural masses (NSM) as paint, sealants, rivets and manholes are represented by specific masses (area and length applied) added to the element properties. NSMs like trailing and leading edges, fuel or payload as well as components as galleys or landing gear are represented as single point masses, which are connected via rigid boundary elements to the primary structure.

The sizing process of SAM consists of the FE preprocessor, the FE solver, the sizing routine itself and the FE post-processor, which are called step by step by the sizing process in a loop until the weight reaches convergence.

In the pre-processing part the resulting pressure distribution (c_P) from the aerodynamic calculation with HISSS is transferred to discrete loads on the FE-model nodes via a node projection method (detailed in [7]). All point masses are converted via the load case specific acceleration to nodal loads. With this data set an implemented FE-solver or alternatively NASTRAN® calculates stresses for every element (σ_x, σ_y, τ_{xy}). The von Mises (v.M.) stresses are used for isotropic materials to size the model (increasing wall thicknesses and section parameters) by the principia of fully stressed design (FSD, [7]). Equation 1 shows exemplary the FSD principia for an isotropic shell element.

$$t_{new} = \begin{cases} t_{old} \cdot \left(c_1 \sqrt{\sigma_e / \sigma_a} \right) & \sigma_e < \sigma_a \\ t_{old} \cdot \left(c_2 + \sqrt{\left(\sigma_e / \sigma_a \right)^2 - 1} \right) & \sigma_e > \sigma_a \end{cases} \qquad (1)$$

with damping coefficients $c_1=0.99$ and $c_2=1.1$

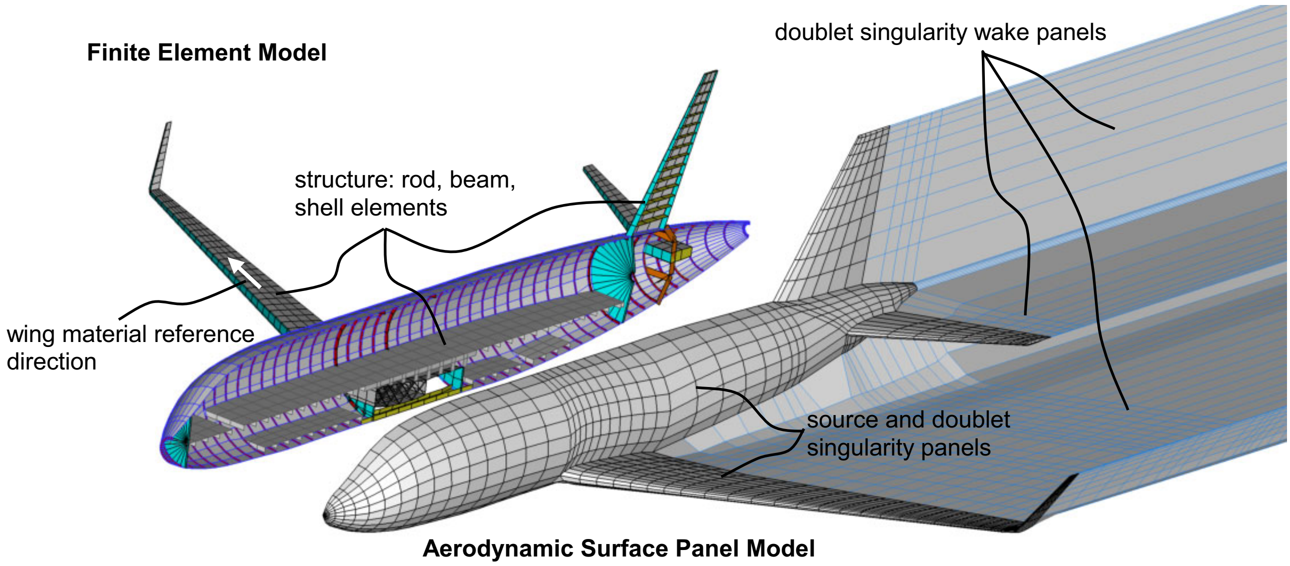

Fig. 3: Example for a parametric aerodynamic model and its corresponding FE model

The new wall thickness is computed from the ratio of the existing v.M. stress to the allowable stress for this element type multiplied by the old thickness. To avoid extreme oscillating thickness changes *Österheld* [7] embedded the stress ratios into square root functions and added the damping factors c_1 and c_2. In addition an upper and lower limit for the wall thickness may be set for every element type so that other design requirements can be considered, which are not represented by a linear static FE analysis and the coarse mesh. A similar procedure is defined for rod (e.g. representing caps) and beam (e.g. representing frames) element types.

The iterative sizing process stops, if the mass change is lower than a limit, or a fixed number of iterations are reached. Finally the post-processor calculates the masses of the single components listed before by analyzing the structural FE model data.

It should be mentioned that it is possible to size the model also under consideration of static aeroelastics with a flexible structure (aeroelastic loop, cp. Fig. 2). Therefore the deformation of the completely sized FE model is transferred to the aerodynamic mesh via a spline method by *Harder* and *Desmarais* [15]. An aerodynamic calculation with deformed mesh is performed and the sizing process is started. The loose coupling scheme is iterated until the aeroelastic equilibrium is fulfilled. This procedure highly increases the calculation time (three days instead of 12h) and is for this reason not a standard procedure.

Fig. 3 shows an example for a parameterized short range aircraft, the idealized aerodynamic and its corresponding FE model.

3 SIZING PROCEDURE FOR FRP STRUCTURES

In the field of the world-wide failure exercise (WWFE) 19 different approaches for failure prediction of composite laminates were compared. *Soden* gives in [5] an overview of the WWFE results and what they mean for the researcher and designer. There are still a lot of uncertainties in predicting failure of laminates and there is no criterion which is conservative in every case as demanded in the introduction. Nevertheless, the Puck criterion has been chosen to be integrated into the sizing process. The reasons for this decision are, that Pruck's criterion:

- is one of the favored in WWFE [5]
- has physical background [16]
- differentiates between fiber and matrix failure [16]
- is available as computer code for validation [17, 18].

In the following subchapters Puck's criterion and its integration into the sizer is presented.

3.1 Puck's Failure Criterion for FRPs

The *Puck* criterion as presented in [15, 18] can be related to the fracture type failure criteria, which differentiates not only between fiber failure (FF) and inter fiber failure (IFF) but also between different types of inter fiber failures.

For FF *Puck* recommends a simple criterion, where the fiber parallel stress σ_I is compared to the corresponding strength $R_{||}$ and an exertion $f_{E,F}$ can be defined as:

$$f_{E,F} = \frac{|\sigma_1|}{R_{||}^{\pm}} \quad \begin{cases} \sigma_1 \geq 0 \rightarrow R_{||}^{+} \\ \sigma_1 \leq 0 \rightarrow R_{||}^{-} \end{cases} \tag{2}$$

Tension stresses are related to the tension strength of the UD lamina, while compression stresses are related to the compression strength of the UD lamina. Results, where $f_{E,FB}$ exceeds 1.0, will fail with FF. This criterion is according to *Schürmann* [19] adequate enough for the preliminary design.

The FRP laminates are represented in the FE model as shells with pure membrane properties (cp. chapter 2.2), so Puck's criterion for IFF can be reduced to the 2D problem. According to *Puck* [16] three IFF modes for the plain stress state of a UD lamina can be differentiated. While failure mode A and B could be tolerated under certain circumstances, mode C has to be avoided in every case, because of the destroying effect of wedge generation. For a sizing method, which is integrated into a preliminary design process where local stress concentrations are not reproduced, none of the three failure modes can be tolerated and have hence to be analyzed.

From *Schürmann* [19] the following plain stress formulation for the three IFF modes has been extracted:

Mode A ($\sigma_\perp > 0$):

$$f_{E,IFA} = \sqrt{\left(\left(1 - p^{+}_{\perp\|}\frac{R^{+}_{\perp}}{R_{\perp\|}}\right)\left(\frac{\sigma_2}{R^{+}_{\perp}}\right)\right)^2 + \left(\frac{\tau_{21}}{R_{\perp\|}}\right)^2} + p^{+}_{\perp\|}\frac{\sigma_2}{R_{\perp\|}} \quad (3)$$

Mode B ($\sigma_2 < 0$ and $\sigma_2 < -R^{A}_{\perp\perp}$):

$$f_{E,IFB} = \sqrt{\left(\frac{p^{-}_{\perp\|}}{R_{\perp\|}}\sigma_2\right)^2 + \left(\frac{\tau_{21}}{R_{\perp\|}}\right)^2} + \frac{p^{-}_{\perp\|}}{R_{\perp\|}}\sigma_2 \quad (4)$$

Mode C ($\sigma_2 < 0$ and $\sigma_2 > -R^{A}_{\perp\perp}$):

$$f_{E,IFC} = \left[\left(\frac{\tau_{21}}{2(1+p^{-}_{\perp\perp})R_{\perp\|}}\right)^2 + \left(\frac{\sigma_2}{R^{-}_{\perp}}\right)^2\right] \cdot \frac{R^{-}_{\perp}}{-\sigma_2} \quad (5)$$

Equation (5) is simplified by the coupling of the incline parameters $p^{-}_{\perp\perp}$ and $p^{-}_{\perp\|}$, so that an iterative calculation of the fracture plane angle θ_{fp} is not necessary. With the equations (2) to (5) all information can be calculated to predict a failure of a lamina ($f_{E,IF} > 1.0$).

3.2 Integration into the Sizer

The stress vector $(\sigma_1, \sigma_2, \tau_{21})^T$ is given as a result of the FE solver for each lamina of a shell element and the corresponding material properties are stored in a data base. Here a limitation occurs. The used FE solvers cannot give results for other than shell elements. Rods and beams have to be calculated with isotropic or smeared material properties. With the stress and material data the exertions $f_{E,i}$ for shell elements can be computed depending on the stress state by equation (2) to (5) for every layer of a laminate. The maximum of each exertion is chosen for further sizing. Important for the sizing procedure is only in which layer/ layers the exertion is higher than 1.0. The failure type, FF or IFF, and respectively mode are not regarded in detail in this simple approach. Equation (6) therefore writes for the exertion of a single lamina:

$$f_{E,L} = \max(f_{E,F}, f_{E,IFi}) \quad (6)$$

In order to design still in a conservative manner and to take inaccuracies (e.g. cut-outs, notches, etc.) from the preliminary design modeling and fatigue into account, the allowable stresses are usually reduced by a notch factor K [7, 20], which could be calculated by handbook methods. For CFRP structures an approach has been chosen, where the notch factor K is applied to the exertion $f_{E,L}$, which follows from equation (6).

$$f^{*}_{E,L} = K \cdot f_{E,L} \quad (7)$$

The notch factor K can be defined for different design regions (e.g. lower skin of the wing torsion box with man holes) separately, so that the influence of diverse inaccuracies is represented by specific factors.

The modification of equation (1) for FRP can be written as follows:

$$t_{new,L} = \begin{cases} t_{old,L} \cdot \left(c_1\sqrt{f^{*}_{E,L}}\right) & f^{*}_{E,L} > 1.0 \\ t_{old,L} \cdot \left(c_2 + \sqrt{\left(f^{*}_{E,L}\right)^2 - 1}\right) & f^{*}_{E,L} < 1.0 \end{cases} \quad (8)$$

with damping coefficients $c_1 = 0.99$ and $c_2 = 1.1$

Instead of the stress ratio the modified exertion $f^{*}_{E,L}$ for each layer is inserted in equation (1) and equation (8) is the result. The damping factors and functions are here the same as for isotropic materials. Through the computation of the exertion in layers the new thickness is calculated for each layer separately. This gives the potential to produce specialized laminates with the limitation, that the fiber direction can not be varied. These specialized laminates have normally not the mass ratio as the origin laminate. To guaranty a balanced laminate the pair-wise non 0° or 90° layers (e.g. ±45° layers) are coupled in their thickness, so that the computed maximum thickness of the pair-wise non 0° or 90° layers is adopted for all pair-wise non 0° or 90° layers.

If the mass ratio of a laminate should not be changed, e.g. 25% 0°, 50% ±45° and 25% 90° (i.e. 25/50/25) should be obtained, the calculated thickness of the maximum exerted layer of a laminate is computed and all layers are set to this maximum multiplied with the relation factor of this layer. The relation factor is evaluated once before sizing. The consequences of an obtained fiber direction mass ratio are demonstrated in chapter 5.

The sizing procedure is iterated for every element and every load case. At the end of one sizing cycle the maximum thickness/section property for each element is stored and the FE analysis is started again (cp. Fig. 2). The layer thicknesses of each composite shell element are thereby stored separately.

4 GENERIC SHORT RANGE AIRCRAFT

For the first part of the impact study a generic short range aircraft in conventional tail-aft configuration has been considered. A single aisle, single class cabin layout and two engines are typical for such a regional jet.

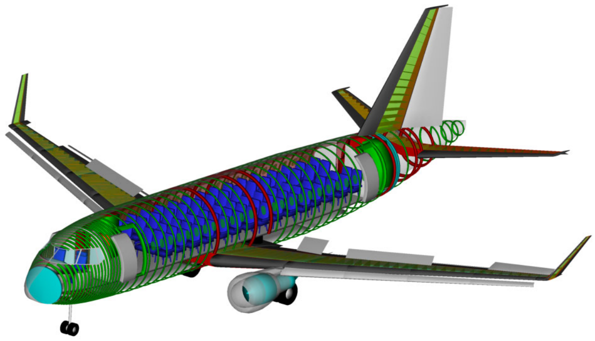

Fig. 4: Parametric Short Range Aircraft Model of PrADO

Fig. 4 gives an example of the visualized global geometry of the baseline configuration.

4.1 Baseline Aircraft Characteristics

Short range aircraft are normally defined as airplanes with an economical range lower than 3000nm (5560km). Here, the requirements for the baseline design are chosen for the design mission as follows:

– range: 1620nm (3000km)
– take off weight: maximum take off weight
– PAX: 70 passengers inclusive luggage
– cabin: single aisle, single class layout
– cruise speed: Ma = 0.80
– altitude at begin of cruise: 10.5km

In **Tab. A 1** the aircraft characteristics as a result of a converged PrADO calculation are depicted for the generic baseline design. As analysis mode the single design has been selected and for the structural mass estimation SAM without aeroelastic loop has been performed. For all primary structure of the baseline design aluminum alloys (cp. **Tab. A 2**) have been assigned. The computed aircraft has a dimension of 28.57m in width, 26.65m in length and 9.35m in height. A thrust of 2x55.6kN is needed for the airplane with 33967kg MTOW to start on a 1807m runway. For the design mission range (3000km) 4805kg fuel at a lift to drag ratio (L/D) of 14.98 are required.

4.2 Impact of CFRP Wing

First, the baseline design has been modified in two versions. Version one, named as CFRP 1, has a primary wing and center box structure of CFRP (cp. Tab. A 2) with a quasi-isotropic (25/50/25) layup at the start of the sizing. The mass ratio but not the direction (0°/±45°/90°; cp. Fig. 3) of the fibers can be designed freely from the sizer (cp. 2.2). Version two, named CFRP 2, has also CFRP with a quasi-isotropic layup for wing and center box, but now the mass ratio is fixed. The only difference between the versions and the baseline design is the material for wing and center box. All other parameters and the thrust of both versions are set identical compared to the baseline design. The impact of these modifications may be examined.

4.2.1 Snow Ball and Layup Effects

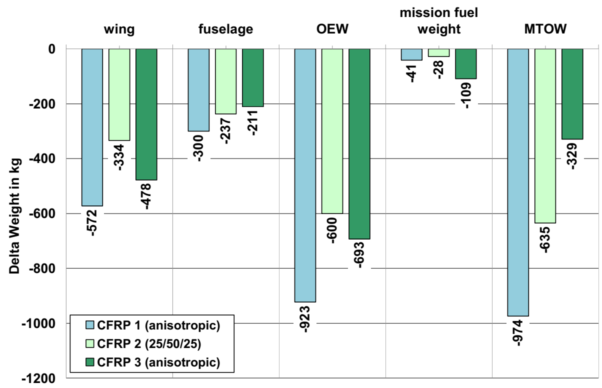

Fig. 5: Impact of Wing Skin Layup on Overall Weight (mass differences compared to baseline design)

In **Fig. 5** the change of characteristic weights against the baseline design are plotted. It can be seen that the difference between the baseline design MTOW (33967kg) and MTOW of the version CFRP 1 (32993kg) with 974kg is not only caused by the pure structural weight benefit (872kg) but also the snow ball effect takes part in the weight gain. The same tendency can be noticed by the weight results of version CFRP 2 and 3. Only by a multidisciplinary process with an iterating character this effect could be reproduced.

For version CFRP 2 the layup have been fixed to quasi-isotropic behavior (25/50/25, cp. Tab. A 2) and it can be noted that the mass benefit is less than for the CFRP 1 version. To give a reason therefore in **Tab. 1** the same element of CFRP 1 and 2 in the upper wing skin inboard the kink are faced (fully converged calculations).

symmetrical layup, 10 layers total		CFRP 1		CFRP 2	
		$t_{overall}$ / mm	3.619	$t_{overall}$ / mm	3.973
		t/ mm	f_E^*	t/ mm	f_E^*
layer 1	0°	0.455	0.891	0.248	0.922
layer 2	+45°	0.300	0.536	0.497	0.541
layer 3	90°	0.300	0.138	0.497	0.124
layer 4	-45°	0.300	0.138	0.497	0.185
layer 5	0°	0.455	0.891	0.248	0.922

Tab. 1: Comparison of the same element in version CFRP 1 and 2 for a the same design load case

The minimum thickness of this element has been defined with t=3mm. The main load direction is in wing longitudinal direction (tension in 0° through wing bending). Cause of the highest exertion in 0° direction, the sizer has reinforced the 0° layers for the CFRP 1 version, so that the exertion is lower 1.0. Through the damping function an exertion of exactly 1.0 cannot be obtained. The layer thickness coupling for ensuring the isotropic property is the reason for the lower utilization in the layers, which point not in the main load direction. In this case the 90° layer has the lowest utilization. The ±45° layers carry a part of the 0° load, but are mainly exerted by shear. The higher overall thickness of the quasi-isotropic layup shows its disadvantage against an adapted layup for this stress state.

4.2.2 Impact on Aircraft Economy

Further the impact on the design mission fuel weight should be lighted, which has a direct impact on the economy. Fig. 5 depicts a fuel weight benefit of only 41kg for version CFRP 1 and 30kg for CFRP 2 although the MTOW is significant lower (CFRP 1: -974kg; CFRP 2: -635kg). Tab. A 1 gives the reason hereof. The L/D at design mission condition for version 1 is 2.11% lower and 1.22% lower for version 2. Corresponding to *Breguet*'s range formula this has a direct proportional influence on the fuel consumption, if cruise speed and specific fuel consumption are constant. The unchanged wing shape is the reason for the lower L/D of the aircraft, which has been optimized for the weight of the baseline aircraft. The lighter versions fly at a lift coefficient too low for this wing design. The dependency of L/D is schematically drawn in **Fig. 6**.

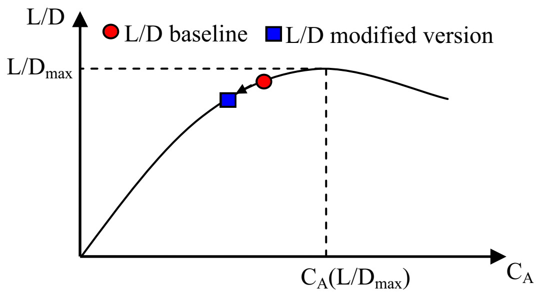

Fig. 6: Relation between L/D and C_A (cp. [3])

There are different starting points for modifying the design, so that the L/D is enhanced for cruise (unchanged Ma number and altitude) and a more economical utilization is possible. According to *Torenbeek* [3] the main impact parameters on the L/D are the wing loading and less the wing aspect ratio:

– The wing loading could be increased by reducing the wing area. But that has a negative effect on the maximum fuel capacity and start and landing behavior.
– MTOW could be increased with advantage to transport more payload. But this is also a disadvantage for the fuel consumption.
– Increasing the wing aspect ratio decreases the induced drag at constant lift [3] and therefore the L/D. But here too the fuel capacity will be decreased and in addition the structure loads are raised through the longer lever arm. The latter effect could be compensated by the higher strength of CFRP.

A possible way to get a more economic aircraft is to increase the MTOW of version CFRP 1 through adding more payload and by increasing the aspect ratio at the same time. Version CFRP 3 is the modified version CFRP 1 with increased payload of 500kg for design mission and an increased aspect ratio of 10%. It can be seen in Tab. A 1 and Fig. 6 that the L/D increases by 1.38% compared to the baseline design and the fuel consumption for design mission decreases by 109kg.

In the next steps the DOCs have to be verified. Therefore, a DOC calculation has been performed corresponding to *Heinze* [6] with the limitation that the same specific costs for aluminum and CFRP wing and center box are assumed. Version CFRP 1 has a benefit of 1.59%, version CFRP 2 of 1.03% and version CFRP 3 of 3.84% compared to the baseline design. The major DOC benefit of version 3 against the baseline design can be explained by the greater amount of payload compared to version 1 and 2. In sum with the lower fuel consumption for the design mission the DOC decreases, so that there is an economical advantage for version CFRP 3.

5 GENERIC LONG RANGE AIRCRAFT

For the second part of the impact study a generic long range aircraft in conventional tail-aft configuration has been planed. A double aisle, three class cabin layout is typical for an intercontinental jet.

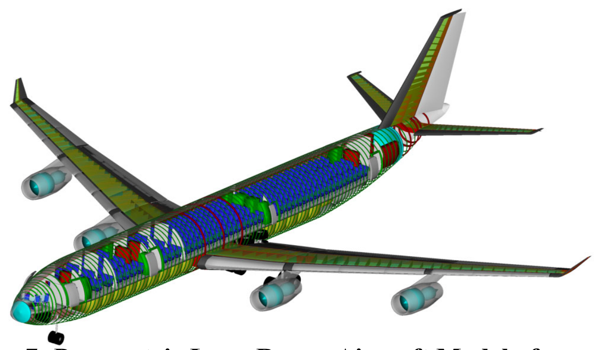

Fig. 7: Parametric Long Range Aircraft Model of PrADO

Fig. 7 gives an example of the visualized global geometry of the baseline long range aircraft powered by four turbofan engines.

5.1 Baseline Aircraft Characteristics

Long range aircraft are normally defined as airplanes with an economical range above 5500nm (10186km). The requirements for the baseline version are selected for the design mission as follows:

– range: 7400nm (13700km)
– take off weight: maximum take off weight
– PAX: 295 passengers inclusive luggage
– cabin: double aisle, three class layout
– cruise speed: Ma = 0.82
– altitude at begin of cruise: 10km

In **Tab. A 3** the aircraft characteristics as a result of a converged PrADO calculation are depicted for the generic baseline design. As analysis mode the single design has been selected and for the structural mass estimation SAM

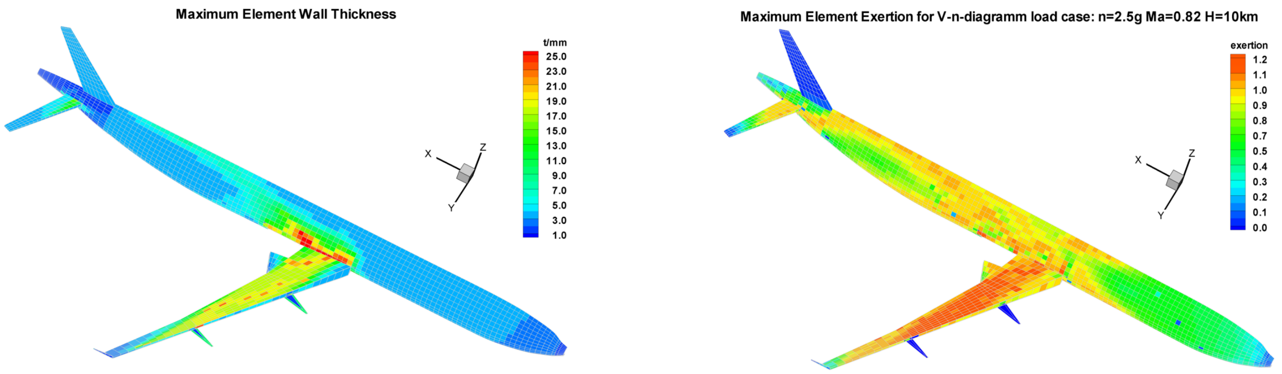

Fig. 8: Wall Thickness and Maximum Element Exertion for CFRP 1

without aeroelastic loop has been performed. For all primary structure of the baseline design aluminum alloys (cp. Tab. A 2) have been assigned. The computed aircraft has a dimension of 60.4m in width, 63.7m in length and 16.4m in height. A thrust of 4x150kN is needed for the airplane with 279443kg MTOW to start on a 3354m runway. For the design mission range (13700km) 104723kg fuel at a L/D of 19.84 are required.

5.2 Impact of CFRP Wing

The baseline aircraft has been modified in three versions. Version one, named as CFRP 1, has a primary wing and center box structure of CFRP (cp. Tab. A 2) with a quasi-isotropic (25/50/25) layup at the start of the sizing. The material reference direction points for the wing in its longitudinal direction (cp. Fig. 3). Version two, named CFRP 2, has also CFRP with a quasi-isotropic layup for wing and center box, but now the mass ratio is fixed. Version three, named CFRP 3, is designed also of CFRP with a 44/44/12 layup for wing and center box and the mass ratio is fixed here, too. The 44/44/12 layup is often used for aeroelastic tailoring [22, 23] as base laminate and therefore its impact on the overall aircraft should be examined, but without performing the aeroelastic loop. The only difference between the versions and the baseline design is the material for wing and center box. All other parameters and the thrust of the three versions are set identical compared to the baseline design. The impact of these modifications should be examined furthermore.

5.2.1 Sizing Results

Fig. 8 illustrates in the left part version the wall thickness exemplary for the CFRP 1. In the right part the maximum element exertion for a V-n-diagram load case (point D), which is most important for sizing of this configuration, is given. For isotropic materials the stress ratios ($\sigma_{e,v.M.}/\sigma_a$, fuselage) and for composite materials the calculated exertions ($f_{E,L}^*$, wing) are depicted. The depicted exertions show on the one hand where the higher loaded areas of this configuration are and on the other hand that the exertions through the sizing method could be set to 1.0 ±0.15 (deviation through the damping function). Areas, where significant lower exertions exist, are defined by the minimum wall thickness boundary condition (e.g. front part of fuselage). Thereby the exertions correlate with the wall thicknesses of the left part of Fig. 8. The VTP is only loaded in x-direction in this symmetric model and thus is mainly defined by minimum wall thickness.

5.2.2 Snow Ball and Layup Effects

The same effect as on the short range aircraft modifications could be seen in **Fig. 9** on the long range aircraft CFRP versions: The mass benefit on OEW and MTOW is larger than the pure gain through lighter structure, which is represented by the iterative process of PrADO.

Furthermore in Fig. 9 the influence of the selected layup for the wing structure can be seen. The highest mass benefit is attained by version CFRP 1, where the mass ratio of the layers can be freely designed by the sizer with the exception that symmetry and balance are obtained. A benefit of 31% for CFRP 1, 14% for CFRP 2 and 28% CFRP 3 wing mass, depending on layup, seems to be within reach compared to analysis made during the NASA AST Composite Wing Program [21], where weight savings of 29-32% for a wing structure have been investigated in a trade off study.

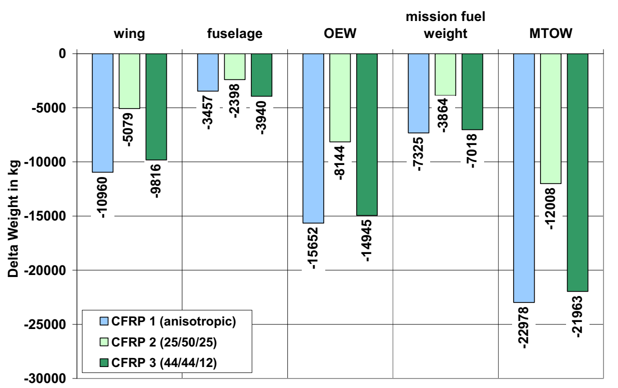

Fig. 9: Impact of Wing Skin Layup on Overall Weight (mass differences compared to baseline design)

In the direct comparison of CFRP 1 with CFRP 3 can be noticed that the mass benefits are similar. A look on the wing tip displacement as quantity for stiffness shows nearly no z-translation difference (0.25%) and no twist difference between CFRP 1 and 2 for the same load case. In detail the wing skin element mass ratios of CFRP 1 differ for the upper skin from root with 40/20/40, to 90/7/3 in the area of the inner engine, to 75/20/5 in the area of the outer engine and to 44/37/19 in the outer wing area. On the lower skin a similar effect can be identified but with more mass percentages of the ±45° layers. But the relatively low mass benefit does not legitimate the very different laminate layup of CFRP 1, because on the one hand a 90/7/3 laminate is more specially designed for the considered load cases, which have to be limited in number in the preliminary design, than the 44/44/12 laminate. On the other hand the manufacturing would be more expensive. A constant 44/44/12 layup with varying laminate thickness should here be the preferred choice.

The version CFRP 2 with fixed quasi-isotropic layup has the lowest mass benefit, because a load adapted single layer thickness could not be realized. Hence, an improvement of 4.3% less MTOW could be achieved, which is a result of the density and strength advantage against aluminum (cp. Tab. A 2).

5.2.3 Impact on Aircraft Economy

Here too the DOC calculation has been performed with the limitation that the same specific costs for aluminum and CFRP wing and center box are assumed. Version CFRP 1 has a benefit of 7.6%, version CFRP 2 of 3.8% and version CFRP 3 of 7.4% compared to the baseline design. All versions show a significant improvement, although L/D is lower than L/D of the baseline design. The reduction of mission fuel is caused mainly by the lower MTOWs. A redesign of the wing would bring an additional advantage for the modifications and should be the next approach for an optimization of this configuration.

6 COMPARISON OF SHORT AND LONG RANGE AIRCRAFT RESULTS

In **Fig. 10** the comparison of the short and the long range aircraft weight benefits, compared to their baseline designs, are shown. Furthermore, the impact of CFRP

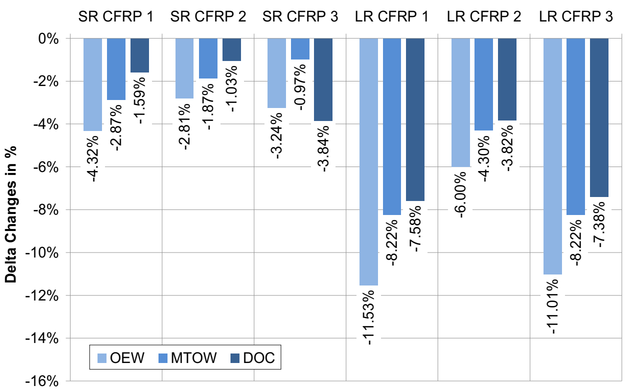

Fig. 10: Comparison of Weight Benefits for Short Range (SR) and Long Range (LR) Aircraft

primary structure for wing and center box on DOC is visualized. First it can be seen that a change of structural weight in general have only less and less impact on MTOW and then on DOC, so that only a significant change of OEW has a moderate impact on DOC. The relatively low weight benefit of the short range aircraft compared to the long range aircraft can be explained by the wall thickness results. These are mainly governed by the minimum limit of 3mm for the short range aircraft wing skin (cp. **Fig. A1**), but are clearly higher than the minimum wall thickness (4mm) for the long range design (cp. Fig. 8). Therefore, the larger weight gain can be seen for the long range design.

Furthermore, the fuel consumption of a long range aircraft has through the longer design mission range a higher impact on the mission fuel weight and therefore on the MTOW [3], so that together with the wall thickness effect a the bigger advantage in DOC results for the long range design.

The comparison of the modified versions has shown the CFRP 3 for the short range design as the most promising modification (cp. 4.2.2) and for the long range design version CFRP 3 (cp. 5.2.3).

7 CONCLUSION

The methodologies of the preliminary aircraft design tool PrADO have been expanded by the functionality to take FRP structures into account. The enhancement of the sizing method for composite materials, analogue to the fully stressed design (FSD) named fully exerted design (FED), has been shown and correlating results to other studies [21] have been presented for two example aircraft designs.

The analysis of both aircraft types has shown that a simple substitution of the structural material should result in a redesign of the aircraft, because weight and aerodynamic design do not correlate in an optimum anymore. Besides, it could be constituted that the weight benefit and the economical advantage is more promising for a long range aircraft. Further, calculations with an aeroelastic loop should be performed to use the full potential of FRP. Therefore an enhancement of the sizing method with respect to fiber orientation would be necessary.

ACKNOWLEDGMENTS

Part of the work was funded by the German aerospace research program (LuFoIII). Special thanks is given to L. Fornasier/ EADS-M for providing the HISSS panel code.

8 REFERENCES

[1] Shirk, M. H.; Hertz, T. J. & Weisshaar, T. A., “Aeroelastic Tailoring - Theory, Practice, and Promise”, J. AIRCRAFT VOL. 23, NO. 1, 6ff., 1986.
[2] Raymer, D. P., “Aircraft Design: A Conceptual Approach”, AIAA; 4.Ed., 2006.
[3] Torenbeek, E., “Synthesis of Subsonic Airplane Design”, Nijhoff, 1982.

[4] Roskam, J., “Airplane Design, Part 1-8”, Design Analysis & Research, 1997.

[5] Soden, P.; Kaddour, A. & Hinton, M., “Recommendations for designers and researchers resulting from the world-wide failure exercise”, Composites Science and Technology 64, 589–604, 2004.

[6] Heinze, W., “Ein Beitrag zur quantitativen Analyse der technischen und wirtschaftlichen Auslegungsgrenzen verschiedener Flugzeugkonzepte für den Transport großer Nutzlasten”, PhD-Thesis TU Braunschweig, ZLR Forschungsbericht 94-01, 1994.

[7] Österheld, C., “Pysikalisch begründete Analyseverfahren im integrierten multidisziplinären Flugzeugentwurf”, PhD-Thesis TU Braunschweig, ZLR Forschungsbericht 2003-06, 2003.

[8] Heinze, W.; Österheld, C. & Horst, P., “Multidisziplinäres Flugzeugentwurfsverfahren PrADO-Programmentwurf und Anwendung im Rahmen von Flugzeug-Konzeptstudien“, in 'Jahrbuch der DGLR-Jahrestagung 2001 in Hamburg', 2001.

[9] Hansen, L. U.; Heinze, W. & Horst, P., “Blended Wing Body Structures in Multidisciplinary Pre-Design”, Structural and Multidisciplinary Optimization 36, 93-106, 2008.

[10] Werner-Westphal, C.; Heinze, W. & Horst, P., “Multidisciplinary Integrated Preliminary Design Applied to Unconventional Aircraft Configurations”, Journal of Aircraft 45, 581-590, 2008.

[11] Horstmann, K-H., “Ein Mehrfach-Traglinienverfahren und seine Verwendung für Entwurf und Nachrechnung nichtplanarer Flügelanordnungen“, PhD-Thesis TU Braunschweig, DFVLR-Forschungsbericht 87-59, 1987

[12] Fornasier, L., “A Higher-Order Subsonic/Supersonic Singularity Method for Calculating Linearized Potential Flow”, 23rd Aerospace Science Meeting & Ehibit, Reno, AIAA 84-1646, 1984.

[13] Burt, M. & Phillips, J., “Prediction of Fuselage and Hull Structure Weight”, Technical report, 1952, RAE Report Structures 122.

[14] Driggs, I. H., “Aircraft Design Analysis Methods as Employed by the Research Division of the Bureau of Aeronautics U.S. Navy Department”, 1949, U. S. Department of the Navy.

[15] Harder, R.L., Desmarais, R.N., “Interpolation using Surface Splines”, Journal of Aircraft, No. 9 (1972), p. 189-197

[16] Puck, A. & Schürmann, H., “Failure analysis of FRP laminates by means of physically based phenomenological models”, Composites Science and Technology 62 (2002) 1633–1662 62, 1633-1662.

[17] Weber, T., „AlfaLam Version 1.1“, www.klub.tu-darmstadt.de, 2006.

[18] NN., „COMPOSITOR“, www.ikv.rwth-aachen.de, 2008.

[19] Schürmann, H., „Konstruieren mit Faser-Kunststoff-Verbunden“, 2. bearbeitete und erweiterte Auflage, Springer, 2007.

[20] Dugas, M. ,“Ein Beitrag zur Auslegung von Faserverbundtragflügeln im Vorentwurf“, PhD thesis, 2002, Universität Stuttgart.

[21] Karal, M.,”AST Composite Wing Program - Executive Summary”, Technical report, The Boeing Company, Long Beach, California, NASA/CR-2001-210650, 2001.

[22] Nagel, B.; Monner, H. P. & Breitbach, E. ,“Aerolastic Tailoring Transsonischer Tragflügel auf Basis Anisotroper und Aktiver Strukturen“, in 'Deutscher Luft- und Raumfahrt Kongress 2004, Dresden'.

[23] Guo, S., “Aeroelastic optimization of an aerobatic aircraft wing structure”, Aerospace Science and Technology 11 (2007) 396–404 11, 396-404.

9 ANNEX

Abbr.	Unit	PrADO Data baseline	PrADO Data CFRP 1	PrADO Data CFRP 2	PrADO Data CFRP 3
B	m	28.57			
L	m	26.65			
H	m	9.35			
S	kN	2x55.6			
Ma_C	-	0.80			
payload	kg	70 PAX = 6510			70 PAX = 6510 +500
maximum payload	kg	9363			
design range	km	3148			
take off field length	m	1807	1700	1737	1734
OEW	kg	21388	20465	20788	20695
mission fuel weight	kg	4806	4765	4778	4697
MTOW	kg	33967	32993	33332	33638
MLW	kg	32166	31220	31551	31633
L/D_C	-	14.98	14.67	14.80	15.19
DOC	€/Skm	0.039974	0.039349	0.039565	0.038497

Tab. A 1: Short Range Aircraft Characteristics

Material	E_1	E_2	ν_{21}	G	$R_{\parallel}^{+}$	$R_{\parallel}^{-}$	$R_{\perp}^{+}$	$R_{\perp}^{-}$	$R_{\perp\parallel}$	ρ
	N/mm²	N/mm²	-	N/mm²	N/mm²	N/mm²	N/mm²	N/mm²	N/mm²	kg/m³
aluminum alloy	73800	73800	0.330	27600	430	430	430	430	109	2854
UD layer*	130000	4650	0.350	4650	1320	840	55	120	75	1570
25/50/25**	48775	48775	0.296	18822	-	-	-	-	-	1570
*prepreg HTA/ 977-2 **calculated with classical laminate theory										

Tab. A 2: Material Properties

Abbr.	Unit	PrADO Data baseline	PrADO Data CFRP 1	PrADO Data CFRP 2	PrADO Data CFRP 3
B	m	60.4			
L	m	63.7			
H	m	16.4			
S	kN	4x150			
Ma_C	-	0.82			
payload	kg	295 PAX = 28615			
maximum payload	kg	50100			
design range	km	13700			
take off field length	m	3554	2911	3203	2936
OEW	kg	135791	120139	127647	120846
mission fuel weight	kg	104723	97975	101160	98257
MTOW	kg	279443	256465	267435	256465
MLW	kg	198045	181441	189403	182191
L/D_C	-	19.84	19.38	19.60	19.40
DOC	€/Skm	0.034040	0.031643	0.032788	0.031701

Tab. A 3: Long Range Aircraft Characteristics

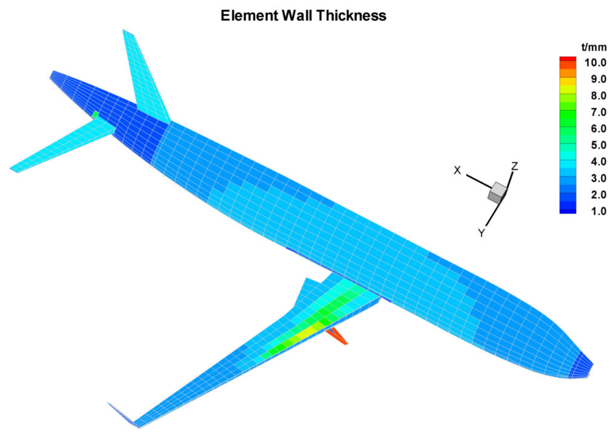

Fig. A1: Wall Thickness Distribution for Short Range Aircraft CFRP 1